AIP Advances

Evidence of quantum correction to conductivity and variable range hopping conduction in nano-crystalline Cu_3N thin film

Cite as: AIP Advances **5**, 107223 (2015); https://doi.org/10.1063/1.4934791
Submitted: 18 September 2015 . Accepted: 13 October 2015 . Published Online: 23 October 2015

Guruprasad Sahoo, and Mahaveer K. Jain

COLLECTIONS

Paper published as part of the special topic on Chemical Physics, Energy, Fluids and Plasmas, Materials Science and Mathematical Physics

View Online Export Citation CrossMark

ARTICLES YOU MAY BE INTERESTED IN

Controlled bipolar doping in Cu_3N (100) thin films
Applied Physics Letters **105**, 222102 (2014); https://doi.org/10.1063/1.4903069

Understanding and control of bipolar self-doping in copper nitride
Journal of Applied Physics **119**, 181508 (2016); https://doi.org/10.1063/1.4948244

Synthesis of Cu_2O from CuO thin films: Optical and electrical properties
AIP Advances **5**, 047143 (2015); https://doi.org/10.1063/1.4919323

© 2015 Author(s).

Evidence of quantum correction to conductivity and variable range hopping conduction in nano-crystalline Cu_3N thin film

Guruprasad Sahoo[a] and Mahaveer K. Jain
Department of Physics, Indian Institute of Technology Madras, Chennai, 600036, India

(Received 18 September 2015; accepted 13 October 2015; published online 23 October 2015)

We have investigated the temperature dependent carrier transport properties of nano-crystalline copper nitride thin films synthesized by modified activated reactive evaporation. The films, prepared in a Cu-rich growth condition are found to be highly disordered and the carrier transport in these films is mainly attributed to the impurity band conduction. We have observed that no single conduction mechanism is appropriate to elucidate the carrier transport in the entire temperature range of 20 – 300 K. Therefore, we have employed different conduction mechanisms in different temperature regimes. The carrier transport of the films in the low temperature regime (20 – 150 K) has been interpreted by implementing quantum correction to the conductivity. In the high temperature regime (200 – 300 K), the conduction mechanism has been successfully analyzed on the basis of Mott's variable range hopping mechanism. Furthermore, it can be predicted that copper ions present at the surface of the crystallites are responsible for the hopping conduction mechanism. © *2015 Author(s). All article content, except where otherwise noted, is licensed under a Creative Commons Attribution 3.0 Unported License.* [http://dx.doi.org/10.1063/1.4934791]

In the recent past, copper nitride (Cu_3N) has been extensively studied as a new age material to be used in variety of applications such as solar cells,[1] optical data storage,[2] magnetic tunnel junctions,[3] resistive switching[4] and fuel cells.[5] Cu_3N crystallizes in a cubic anti-ReO_3 structure (space group *Pm3m*) with lattice parameter 3.819 Å where N atoms occupy corners of the cubic cell and Cu atoms are located at centre of edges.[6] The peculiarity of this structure is the existence of a vacant site at the center of the cubic cell where an external element can be favorably incorporated. A significant amount of work has been carried out, both theoretically and experimentally to study the possibility of incorporating variety of elements such as Cu,[7,8] Ag,[7] Au,[7,9] Zn,[10] Pd,[10,11] In,[10] Fe,Co,Ni[12–14] etc. at the vacant site and their associated changes or modifications in various properties. Apart from this, Cu_3N in its pure form shows diverse and versatile structural, optical and electrical properties which are strongly dependent on stoichiometry of the compound. To cite a few, optical band gap in a wide range from 0.8 to 1.9 eV[3,15–19] and electrical resistivity in the range 10^{-5} to 10^3 Ω cm[10,16–19] have been reported for this material. Interestingly, Cu_3N in both *n* and *p* type configuration can be easily prepared by imposing suitable Cu-rich and N-rich growth conditions respectively,[1,20] acclaiming the immense impact of this material in the field of optoelectronics. Hence, understanding optical and electrical properties of Cu_3N has drawn enormous attention of researchers. Various reports are available demonstrating the electrical properties of Cu_3N.[10,17–20] Nevertheless, the carrier transport mechanism in Cu_3N is not well understood, especially at low temperatures. In order to further improve utility of this material, significant amount of research is needed to understand electrical transport properties. In this report, we aim to investigate the low temperature transport mechanism of nano-crystalline Cu_3N thin films prepared by modified activated reactive evaporation (MARE).

The Cu_3N films under consideration were deposited on glass substrates at room temperature by MARE technique. The MARE technique is a modification over the conventional activated

[a]Author to whom correspondence should be addressed. Electronic mail: guruprasad@physics.iitm.ac.in

 ©Author(s) 2015

reactive evaporation (ARE), where the substrate is intentionally kept on the cathode while it is kept grounded in case of the latter.[21] The details of the growth and characterization of Cu_3N thin films prepared by MARE have been discussed in our previous report,[22] where the films grown at higher deposition pressures were observed to be highly insulating. The films used for the present study were prepared by evaporating Cu in the presence of N_2 plasma generated at 50 W rf power and 1.5 mTorr growth pressure. The glass substrate was fixed on the cathode, at a distance of 10 cm from the evaporation source and the deposition was carried out for 10 min. X-ray diffraction (XRD) for structural characterization were carried out using Panalytical X'Pert Pro X-ray diffractometer with a Cu $K\alpha_1$ (λ = 1.5406 Å) radiation. The scanning electron microscope (SEM) micrographs were taken using a FEI Quanta 400 SEM. The transmission spectra were taken using a Jasco V-570 UV-Vis-NIR spectrophotometer. Ellipsometry measurements were carried out using a J. A. Woollam M-2000VI EC-400 spectroscopic ellipsometer with an incident angle of 70°. Hall Effect measurements in the temperature range of 20 – 300 K were carried out using a Lake Shore Hall effect measurement system in van der Pauw geometry.

XRD pattern of the as-deposited Cu_3N film is shown in Fig. 1(a). The diffraction peaks identified as (100), (111) and (200) planes represent a polycrystalline Cu_3N thin film in cubic anti-ReO_3 structure.[6] Its calculated lattice parameter 3.819 Å exactly matches with the reported values.[6,12] No evidence of secondary metallic Cu phase is observed. The average crystallite size calculated using Debye-Scherrer's formula is found to be 14 nm which accounts for a poor crystallization of the films compared to those prepared at higher deposition pressures as reported earlier.[22] SEM micrograph of the film as presented in Fig. 1(b) shows that small spherical shaped grains are uniformly distributed throughout the surface of the film. However, these grains exhibit a non-uniform size distribution.

Figure 2(a) shows the transmission spectrum of the Cu_3N film where a very low value of transmittance is observed which gradually decreases with decrease in the wavelength. This indicates a highly disorder nature of the film. A very faint absorption edge is observed at ~ 1250 nm, and below this the transmittance drops to zero. Indirect band gap (E_g) was calculated from Tauc's plot[23] using the following expressions.

$$\alpha = \frac{2.303\log(1/T)}{d} \tag{1}$$

$$(\alpha h\nu)^{1/2} = A(h\nu - E_g) \tag{2}$$

Here α is the absorption coefficient, $h\nu$ is the photon energy, T is the transmittance, d is the film thickness and A is proportionality constant. Band gap is determined by plotting $(\alpha h\nu)^{1/2}$ versus $h\nu$ and linearly extrapolating the full line to the abscissa $h\nu$, which is shown in Fig. 2(b). The measured

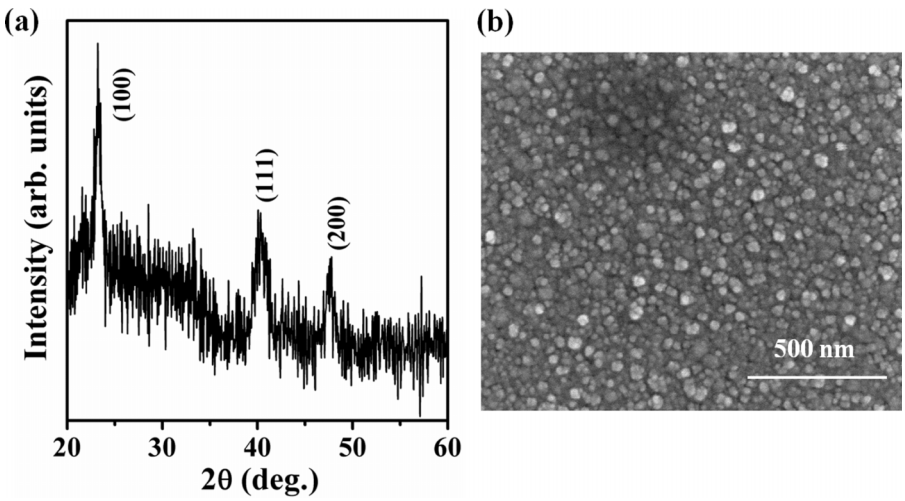

FIG. 1. (a) XRD pattern and (b) SEM micrograph of the Cu_3N film.

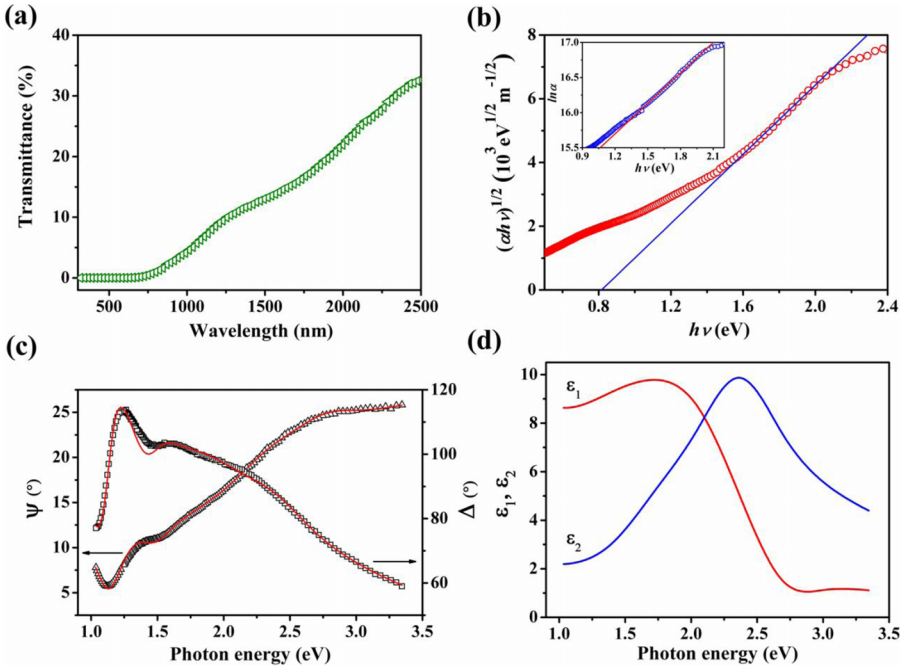

FIG. 2. (a) Transmission spectrum of the Cu_3N film. (b) $(\alpha h\nu)^{1/2}$ vs. $h\nu$ plot for the determination of indirect band gap. Inset shows $ln\,\alpha$ vs. $h\nu$ plot for the determination of Urbach energy. (c) Spectroscopic ellipsometry parameters ψ and Δ of the Cu_3N film. (d) Variation of real (ε_1) and imaginary (ε_2) parts of dielectric constant with photon energy.

band gap 0.82 eV of the film is considerably lower than that of the Cu_3N films grown by MARE at higher deposition pressures.[22] This may be due to the fact that the film under consideration is highly disordered one and therefore, there may exist a large number of defect-states in the mid gap region. It is well known that the presence of point defects or structural disorder in a system gives rise to a tailing of density of states (DOS) in the forbidden energy gap, widely known as Urbach tail[24] and the width of the tail is interpreted as Urbach energy (E_u). Higher value of E_u represents higher degree of disorder. Absorption coefficient α is related to E_u as per the following expression.

$$\alpha = \alpha_0 \exp\left(\frac{h\nu}{E_u}\right) \tag{3}$$

Where α_0 is a constant. E_u can be calculated from linear fitting of the plot $ln\alpha$ versus $h\nu$ (inset of Fig. 2(b)); where inverse of the slope gives the value of E_u. The value of E_u is found to be 692 meV which infers that the system under consideration is highly disordered. Spectroscopic ellipsometry parameters, amplitude ratio (ψ) and phase difference (Δ) are illustrated in Fig. 2(c). The real (ε_1) and imaginary (ε_2) parts of the dielectric constant were extracted by analyzing the ellipsometry data and their variations with the photon energy are plotted in Fig. 2(d). The variations of ε_1 and ε_2 with energy are similar to the one reported earlier for Cu_3N.[3]

Fig. 3(a) shows temperature dependent resistivity (ρ) of the Cu_3N film in the range of 20 – 300 K. The resistivity monotonically decreases with increase in the temperature which shows a semiconducting nature of the film. Fig. 3(b) shows carrier concentration (n) and Hall mobility as a function of temperature. We observe high carrier density with very low mobility which remains nearly same over the entire temperature range. From these results, electron wave vector (k_F) and mean free path (l) were calculated using the relations, $k_F = (3\pi^2 n)^{1/3}$ and $l = \hbar k_F / ne^2\rho$, where $\hbar$ and e are Planck's constant and electronic charge respectively.[25] From these calculations it is observed that $(k_F l)^{-1} > 1$, which indicates the high degree of disorder in the system.[25] As a result, the electronic wave functions are expected to be localized and the Fermi energy (E_F) may lie in the range of energies where states are localized. Carrier transport in such a disordered system cannot be explained by the classical Arrhenius equation, $\rho(T) = \rho_0 \exp(E_a/k_B T)$ which accounts for the thermal excitation of carriers, as

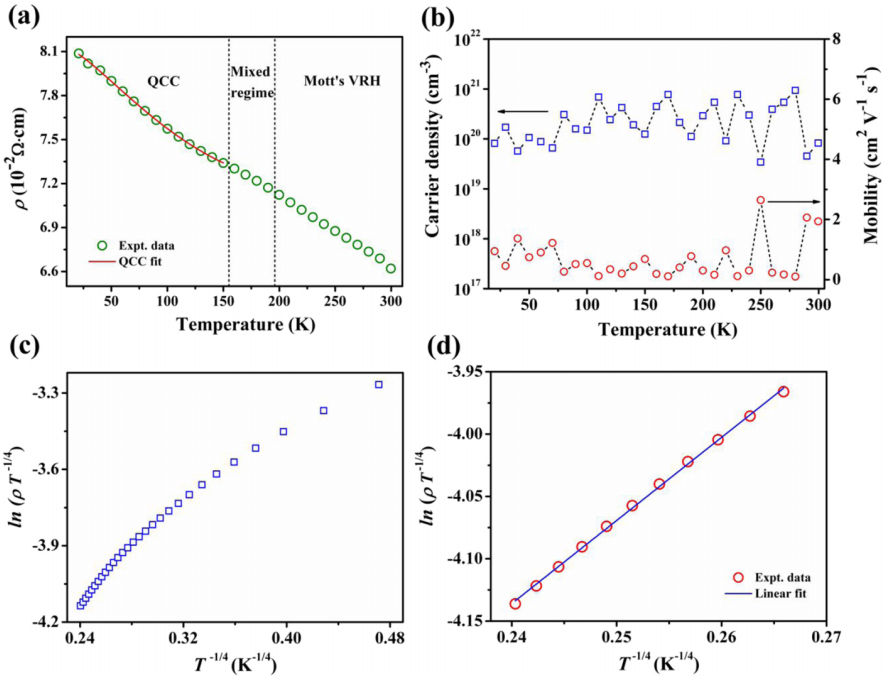

FIG. 3. (a) Temperature dependent resistivity of the Cu_3N film. Solid line represents the QCC fit at lower temperatures (20 – 150 K). (b) Temperature dependent carrier density and Hall mobility of the Cu_3N film. (c) $ln(\rho T^{-1/4})$ vs. $T^{-1/4}$ plot in the entire temperature range. (d) $ln(\rho T^{-1/4})$ vs. $T^{-1/4}$ plot in the high temperature regime (200 – 300 K).

generally observed in intrinsic or lightly doped semiconductors (E_a is the corresponding activation energy and k_B is the Boltzmann constant). In such disorder systems, impurity band conduction; more precisely, hopping conduction mechanism is most likely to occur. In general, there are two types of hopping conduction mechanisms possible in such disordered system; nearest neighbor hopping (NNH) and variable range hopping (VRH).[26] In NNH, charge carriers under the influence of thermal activation jump (hop) over a distance to a nearest neighboring site. In case of VRH, the carriers by absorbing phonons hop from one site to another above the E_F, which has minimum energy difference irrespective of the spatial distance. The typical hopping length in VRH increases with decrease in temperature. However, the validity of occurrence of either NNH or VRH model is determined by the ratio R_0/a_B, where R_0 is the average distance to a nearest neighbor and a_B is the Bohr radius (or localization length). NNH is expected to occur when $R_0/a_B >> 1$. When R_0/a_B is comparable with or less than unity, then VRH conduction is more likely expected.[26] The Bohr radius can be calculated as, $a_B = 4\pi\varepsilon_0\varepsilon\hbar^2/m^*e^2$, where ε_0 is the permittivity of vacuum, ε is the static dielectric constant and m^* is the effective mass. We have calculated $a_B = 1.03$ nm using the value of ε as 9.76, obtained from the ellipsometric measurements (Fig. 2(d)) and reported value of $m^* = 0.5m_0$[1] for Cu_3N. The distance R_0 can be determined using the relation, $R_0 = (3/4\pi n)^{1/3}$. Based on our experimental results, the value of R_0/a_B is calculated to be close to unity and hence we rule out any possibility of NNH conduction and confine ourselves to use VRH model for further analysis of the resistivity plot. Therefore, we tried to implement Mott's 3D VRH model to our resistivity data, according to which the temperature dependent resistivity is expressed as; [26–28]

$$\rho(T) = A_0\, T^{1/4} \exp\left[\left(\frac{T_0}{T}\right)^{1/4}\right] \tag{4}$$

where, A_0 is a prefactor constant and T_0 is the characteristic hopping temperature that depends on the DOS $N(E_F)$ at the Fermi level as follows;

$$T_0 = \frac{21.2}{k_B N(E_F)\xi^3} \tag{5}$$

Here ξ is the localization radius of charge carriers. The plot of $ln(\rho T^{-1/4})$ versus $T^{-1/4}$ has been illustrated in Fig. 3(c). Straight line behavior is observed at higher temperatures which favors the applicability of the VRH model. However, at lower temperatures, deviation from linearity is noticed indicating the invalidation of the VRH model. The $ln(\rho T^{-1/4})$ versus $T^{-1/4}$ plot with linear fitting in the high temperature regime (200 – 300 K) is shown in Fig. 3(d). The corresponding χ^2 (χ is the least-square fit coefficient) is obtained to be 0.999, which accounts for a satisfactory fit. The characteristic temperature T_0, calculated from the slope of the linear fit is found to be 1974 K. It can be seen from the equation (5) that T_0 contains two unknown parameters, $N(E_F)$ and ξ. Therefore, either of them can be calculated provided other is known. Assuming ξ nearly same as the Bohr radius a_B (=1.03 nm), the value of $N(E_F)$ in the HT regime is calculated to be 1.14×10^{23} eV^{-1} cm^{-3}. This value of $N(E_F)$ is very high and comparable to the conduction band states. This high value of $N(E_F)$ can be attributed to the contribution of copper ions present at the surface of the crystallites. In order to verify the same, we have followed a similar procedure as demonstrated by Bose *et al*.[29] The number of states that contribute to the electrical conductivity at room temperature, T_r = 300 K is calculated to be 2.96×10^{21} cm^{-3} (obtained by multiplying k_BT_r with $N(E_F)$. In the next, we calculated the concentration of Cu ions present at surface of the crystallites as follows. Using the molecular mass (204.63 g/mol) and density (5.84 g cm^{-3}) of Cu_3N[18], and assuming an average diameter of 14 nm for a spherical shaped Cu_3N nano-crystallite, the number of Cu_3N molecules in the crystallite can be calculated as $\sim 2.47\times10^4$. Therefore, number of Cu ions in one crystallite is $\sim 7.41\times10^4$. Since, volume of a crystallite is calculated as $\sim 1.437\times10^{-18}$ cm^3, we estimate the number of Cu_3N crystallites in unit volume ($1cm^{-3}$) to be 6.96×10^{17}. As a result, the concentration of Cu ions in the nano-crystallites will be $\sim 5.15\times10^{22}$ cm^{-3}. In the present system, if we believe Cu ions present at interfaces only contribute to the conductivity, then the concentration of such ions is about 10 % of the concentration in nano-crystallites, i.e. 5.15×10^{21} cm^{-3}. Hence, we assume that the number of localized states formed by interfacial Cu ions is nearly close to the number of states that contribute to the electrical conductivity at T_r (2.96×10^{21} cm^{-3}) calculated using the VRH model. These are the band states that are localized due to disorder at the interfaces and contribute to the hopping conduction. In an earlier report, Mott's VRH has been observed in Cu_3N films where it is mentioned that Cu-terminated (111) planes provide alternative hopping paths for charge carriers.[7] Since the films under consideration were prepared in a Cu-rich condition, it can be suspected that some Cu atoms may fill the vacant sites of regular Cu_3N lattice. Experimental[7] as well as theoretical[8] investigation suggests a significant lattice expansion on insertion of Cu atoms into the vacant sites. However, the obtained lattice parameter in the present case exactly matches to that of a pure Cu_3N as mentioned earlier; therefore, we do not expect Cu atoms filling the vacant sites.

Though, the Mott's VRH model satisfactorily explains the conduction mechanism at higher temperatures, the data in the lower temperatures could not be interpreted using the same model. The phonon energy at lower temperatures is insufficient to initiate hopping of carriers. As an alternate, we have tried to implement quantum correction to conductivity (QCC) which is an appropriate model for the interpretation of resistivity upturn at low temperatures for disorder systems.[25] Two mechanisms that lead to the QCC are; the localization effect which arises due to the self-interference of quantum wave functions backscattered on impurities and the electron-electron interaction (EEI).[25] The temperature dependent resistivity after considering QCC takes the form:-

$$\rho(T) = \frac{1}{\sigma_0 + \sigma_1 T^{1/2} + \sigma_2 T^{p/2}} + kT^2 \tag{6}$$

where, $\sigma_0(= 1/\rho_0)$ is the residual conductivity, $\sigma_1 T^{1/2}$ corresponds to the EEI and $\sigma_2 T^{p/2}$ represents the contribution due to localization, in which p depends on the nature of interaction (p = 2 or 3 for electron-electron or electron-phonon interactions respectively). The localization term reduces conductivity at lower temperatures, because the scale of interference increases as temperature reduces. In addition to the quantum corrected resistivity term, a term kT^2 is included which accounts for the high temperature electron-electron scattering contribution. The resistivity data fitted with equation (6) in the low temperature regime (20 – 150 K) is represented in Fig. 3(a). The best fit is obtained by picking the parameter p as 2 which means that the electron-electron interaction plays the dominating role. The fitted values of the parameters σ_0, σ_1, σ_2 and k are found to be 12.50±0.09 $(\Omega\ cm)^{-1}$,

-0.129 ± 0.03 $(\Omega\ \text{cm})^{-1}\ \text{K}^{-1/2}$, 0.023 ± 0.003 $(\Omega\ \text{cm K})^{-1}$ and $1.64\times10^{-7}\pm2.55\times10^{-8}$ $(\Omega\ \text{cm})\ \text{K}^{-2}$ respectively. Though QCC in general is applicable at very low temperatures ($T < 10$ K), however various reports show satisfactory implementation of QCC at considerably higher temperatures.[30,31]

In conclusion, the electrical transport properties of nano-crystalline Cu_3N thin films were studied at low temperatures. The condition $(k_F l)^{-1} > 1$, meant for disorder systems has been verified for the films under consideration. The carrier transport at low temperatures (20 – 150 K) has been interpreted by implementing quantum correction to the conductivity. For higher temperatures (200 – 300 K), the conduction mechanism is elucidated on the basis of Mott's variable range hopping mechanism where the DOS at the Fermi level $N(E_F)$ is calculated to be in the order of 10^{23} eV^{-1} cm^{-3}. It can be presumed that copper ions present at surface of the crystallites contribute to such a large value of DOS and are responsible for the hopping conduction.

Authors thank Dr. A. Subrahmanyam, department of Physics, IIT Madras for the Hall effect measurements.

[1] A. Zakutayev, C. M. Caskey, A. N. Fioretti, D. S. Ginley, J. Vidal, V. Stevanovic, E. Tea, and S. Lany, J. Phys. Chem. Lett. **5**, 1117 (2014).
[2] M. Asano, K. Umeda, and A. Tasaki, Jpn. J. Appl. Phys. **29**, 1985 (1990).
[3] D. M. Borsa, S. Grachev, C. Presura, and D. O. Boerma, Appl. Phys. Lett. **80**, 1823 (2002).
[4] Q. Lu, X. Zhang, W. Zhu, Y. Zhou, Q. Zhou, L. Liu, and X. Wu, Phys. Status Solidi A **208**, 874 (2011).
[5] N. Pereira, L. Dupont, J. M. Tarascon, L. C. Klein, and G. G. Amatucci, J. Electrochem. Soc. **150**, A1273 (2003).
[6] U. Zachweija and H. Jacobs, J. Less Common Met. **161**, 175 (1990).
[7] N. Lu, A. Ji, and Z. Cao, Sci. Rep. **3**, 3090 (2013).
[8] M. G. Moreno-Armenta, A. Martínez-Ruiz, and N. Takeuchi, Solid State Sci. **6**, 9 (2004).
[9] G. Soto, I. Ponce, M. G. Moreno, F. Yubero, and W. D. Cruz, J. Alloys Compd. **594**, 48 (2014).
[10] A. Ji, D. Yun, L. Gao, and Z. Cao, Phys. Status Solidi A **207**, 2769 (2010).
[11] U. Hahn and W. Weber, Phys. Rev. B **53**, 12684 (1996).
[12] X. Y. Fan, Z. J. Li, A. L. Meng, C. Li, Z. G. Wu, and P. X. Yan, J. Phys. D: Appl. Phys. **47**, 185304 (2014).
[13] J. Yang, S. Huang, Z. Wang, Y. Hou, Y. Shi, J. Zhang, J. Yang, and X. Li, J. Vac. Sci. Technol. A **32**, 051510 (2014).
[14] H. Chen, X. Li, J. Zhao, Z. Wu, T. Yang, Y. Ma, W. Huang, and K. Yao, Comp. Theor. Chem. **1027**, 33 (2014).
[15] S. Ghosh, F. Singh, D. Choudhary, D. K. Avasthi, V. Ganesan, P. Shah, and A. Gupta, Surf. Coat. Technol. **142–144**, 1034 (2001).
[16] J. F. Pierson, Vacuum **66**, 59 (2002).
[17] G. H. Yue, P. X. Yan, J. Z. Liu, M. X. Wang, M. Li, and X. M. Yuan, J. Appl. Phys. **98**, 103506 (2005).
[18] T. Nosaka, M. Yoshitake, A. Okamoto, S. Ogawa, and Y. Nakayama, Thin Solid Films **348**, 8 (1999).
[19] D. Wang, N. Nakamine, and Y. Hayashi, J. Vac. Sci. Technol. A **16**, 2084 (1998).
[20] K. Matsuzaki, T. Okazaki, Y. Lee, H. Hosono, and T. Susaki, Appl. Phys. Lett. **105**, 222102 (2014).
[21] K. P. Biju, A. Subrahmanyam, and M. K. Jain, J. Phys. D: Appl. Phys. **41**, 155409 (2008).
[22] G. Sahoo, S. R. Meher, and M. K. Jain, Mater. Sci. Eng. B **191**, 7 (2015).
[23] J. Tauc, R. Grigorovici, and A. Vancu, Phys. Status Solidi B **15**, 627 (1966).
[24] F. Urbach, Phys. Rev. B **92**, 1324 (1953).
[25] P. A. Lee and T. V. Ramakrishnan, Rev. Mod. Phys. **57**, 287 (1985).
[26] N. F. Mott and E. A. Davis, *Electron Processes in Non-Crystalline Materials* (Clarendon, Oxford, 1979).
[27] B. I. Shklovskii and A. L. Efros, *Electronic Properties of Doped Semiconductors* (Springer, Berlin, 1984).
[28] K. G. Lisunov, M. Guk, A. Nateprov, S. Levcenko, V. Tezlevan, and E. Arushanov, Sol. Energy Mater. Sol. Cells **112**, 127 (2013).
[29] A. Bose, S. Basu, S. Banerjee, and D. Chakravorty, J. Appl. Phys. **98**, 074307 (2005).
[30] V. P. Arya, V. Prasad, and P. S. A. Kumar, J. Phys.: Condens. Matter **24**, 245602 (2012).
[31] S. R. Meher, R. V. M. Naidu, K. P. Biju, A. Subrahmanyam, and M. K. Jain, Appl. Phys. Lett. **99**, 082112 (2011).